Integrated Learning and Optimization for Ramping Cost Minimization with Load Demand and Wind Generation Control in Real-Time Electricity Market

Imran Pervez[a], Omar Knio[a,*]

[a]*Computer, Electrical, and Mathematical Sciences and Engineering Division,King Abdullah University of Science and Technology, Thuwal, 23955, Makkah, Saudi Arabia*

Abstract

We developed a new integrated learning and optimization (ILO) methodology to predict context-aware unknown parameters in economic dispatch (ED), a crucial problem in power systems solved to generate optimal power dispatching decisions to serve consumer load. The ED formulation in the current study consists of load and renewable generation as unknown parameters in its constraints predicted using contextual information (e.g., prior load, temperature). The ILO framework train a neural network (NN) to estimate ED parameters by minimizing an application-specific regret function which is a difference between ground truth and NN-driven decisions favouring better ED decisions. We thoroughly analyze the feasible region of ED formulation to understand the impact of load and renewable learning together on the ED decisions. Corresponding to that we developed a new regret function to capture real-time electricity market operations where differences in pre-

*Corresponding author.

Email addresses: imran.pervez@kaust.edu.sa (Imran Pervez), omar.knio@kaust.edu.sa (Omar Knio)

dicted and true loads are corrected by ramping generators in real-time but at a higher cost than the market price. The proposed regret function when minimized using ILO framework train the NN to guide the load and renewable predictions to generate ED decisions favouring minimum generator ramping costs. This is unlike conventional sequential learning and optimization (SLO) framework which train NN to accurately estimate load and renewable instead of better ED decisions. The combined training of load and renewable using ILO is a new concept and lead to significantly improved ramping costs when compared with SLO based training of load and renewable and SLO trained load with 100% accurate renewable proving its decision-focused capability.
Keywords: Integrated learning and optimization, sequential learning and optimization, economic dispatch, line congestion

1. Introduction

The transition to renewable energy sources is fraught with difficulties, such as a high rate of frequency change, netload (demand minus renewable generation) below base load, the requirement for quick ramping generators, the relatively high capacity of non-dispatchable sources, difficulties with forecasting and prediction, and lower revenue recovery (market price minus production cost) of conventional generators, which results in noticeably higher production prices during peak or mid-peak hours. In addition, there is a growing degree of unpredictability in the load demand, as seen by the introduction of new consumption profiles by electric vehicles (EVs) and the rise in loads brought on by large data centers and industry electrification.

For electricity systems to operate in an economical and dependable man-

ner, the aforementioned issues must be resolved. The economic dispatch (ED) optimization problem is fundamental to the operation of reliable and cost-effective power systems. In an optimal scenario, the ED problem generates power-dispatching decisions based on a variety of forecasts, such as load demand, renewable generation, and power transfer distribution factors (PTDF).

One important application of power systems is the electrical market mechanism, which determines production and consumption schedules and pricing. The energy market's operations are heavily reliant on ED/DCOPF choices, which are based on a variety of forecasts, such as load demand and renewable technology generation. Inaccurate predictions propagate via optimization difficulties, resulting in inaccurate dispatch decisions that may have a major influence on market operations and revenues.

There are several forms of electricity markets, including the day-ahead market (DAM), intraday market (IDM), and real-time market. The current study focuses on DAM and RTM, with the former scheduling market decisions prior to real-time operation based on various projections and the latter scheduling real-time market operations.

Because the DAM or other future market transactions rely on weather, load, renewable, and other forecasts, actual production and consumption from renewables and loads are likely to deviate from market-cleared schedules in real time, resulting in a supply-demand imbalance or line congestion.

Independent system operators (ISOs) use RTM techniques to balance supply and demand in near-real-time to avoid user discomfort, blackouts, or abrupt demand cutbacks. The IDM and BM mechanisms tackle ED prob-

lems in real-time by making purchasing/selling decisions for electricity from different market traders eager to generate/consume more in order to ramp up/down overall system power for total supply and demand balance and line congestion improvement. Inaccuracies in forecasts result in increased fees for deviations from nominations, raising overall system costs.

In general, the ED problem is addressed in three steps: i) training phase: a prediction model is trained using historical data, including context and parameters required within ED and DCOPF; ii) prediction phase: given a specific context, the prediction model is applied to predict parameters for the ED or DCOPF problems; and iii) optimization phase: the ED or DCOPF problems are solved by parameterizing them over the parameters determined in the prediction phase. This is known as sequential learning and optimization (SLO) [1]. A different method adheres to the three stages of SLO, but it adds two components to the training phase: a) the optimization issue from the optimization phase; and b) a loss function to quantify deviations depending on post-optimization choices. The term integrated learning and optimization (ILO) [1] refers to this methodology. The primary focus of this work is the application of ILO to ED and DCOPF and its performance analysis. The text demonstrates the superiority of the ILO over the SLO and further elaborates these ideas, specifics, and methodology.

1.1. Literature overview

Three primary topics that are pertinent to this work are covered in the literature review. The first focuses on learning algorithms created to forecast pertinent parameters in applications involving power systems. The second discusses model predictive control-based stochastic optimization techniques

for ED problems. Lastly, we concentrate on the topic of this study, which is ILO applications and advancements. These three fields offer pertinent techniques for parameter prediction and optimization problems that deal with crucial decision-making issues including assuming values for context-dependent and unknown parameters.

Various supervised learning algorithms have been proposed in the literature for training predictions in the ED/DCOPF optimization setting. To increase the accuracy of load prediction, the authors in [2] employed a Levenberg–Marquardt back-propagation (LM-BP) neural network (NN). To guarantee greater speed, precision, and stability, the gradient descent and quasi-Newton methods are combined. The authors in [3] employed look-ahead window (prediction horizon) size selection for look-ahead (multi-time) load forecasting and auto-machine learning (auto-ML) for feature extraction. They demonstrate how optimizing hyperparameter selection can increase overall forecasting/prediction accuracy. In [4], the authors suggested a temporal fusion transformer (TFT) and transfer learning strategy to train prediction models for buildings and users using tiny load consumption data sets. Despite the limited amount of data available, the trained model offers a notable increase in accuracy when compared to current methods.

The authors in [5] extracted features from the data using an unsupervised learning approach and a deep neural network. A deep convolutional neural network (DCNN), which employs convolutional layers and additional dense layers to produce precise load prediction accuracy, was proposed in [6]. In [7], the authors presented a hybrid approach that use long short term memory (LSTM) to extract patterns from the time-series data and convolutional neu-

ral networks (CNN) to construct the load trend learning capability. In [8], a load prediction approach based on Gaussian processes (GP) was proposed. In order to handle the high dimensional data, the suggested GP regression model uses compositional kernels, which assign weights to the most significant input features. High data dimensionality is addressed by training with the most crucial features, which also improves overall prediction accuracy.

For load prediction, the authors in [9] suggested a homogenous ensemble-based approach (random forest (RF)). Additionally, the authors examined the significance of several dataset properties. In terms of accuracy, the RF algorithm as a whole fared better than other algorithms. To create an additive model that minimizes the loss/regret function, the authors in [10] employed a gradient boosting (GB) approach, which iteratively merges multiple weak models (less accurate) through numerical optimization. It was discovered that the suggested approach increased the accuracy of load prediction. In order to determine the ideal feature space, the authors in [11] suggested a vector field-based support vector regression technique that uses a vector field to map a high-dimensional feature space. The proposed algorithm improved the accuracy and robustness of the load prediction. Though the above-mentioned methods improved the prediction accuracy, none of them trained the predictions to learn better decisions on parameters that minimizes a regret function.

There have been a lot of deep learning algorithms published for wind forecasting explained in a review published in [40]. In [41] adopted a CNN to extract features and then used LSTM for short-term prediction. Extending the LSTM cell through peephole connections solves the problem that when the LSTM closes the output gate, the gate cannot obtain any information

from the output of the storage unit, bringing better prediction effects [42]. Authors in [43] proposed LSTM-EFG, which enhances the effect of forgetting the door and improves the activation function. The shared weight long short-term memory network model is introduced to reduce the training time and the variables that need to be optimized [44]. An LSTM-Ms model was designed to use feed-forward neural networks to construct rougher time-scale sequences than the original model and then used LSTM to process these sequences [45]. Through LSTM-Ms, it is easier to learn the long-term dependence of wind speed sequence. In [46], the authors employed a newmethod, namely long short-term memory network based on neighbourhood gates (NLSTM), which dynamically adjusts the network structure according to the specific equivalent tree causality to handle the complex causality in wind speed prediction, thereby improving the accuracy of prediction. Excessive stacking of LSTM units may lead to a decrease in training accuracy and efficiency. Lopez et al.Authors in [47] found a better starting point for training by evaluating a number of instances and using these output signals to perform a ridge regression to obtain the output layer weights. Generally, the high-frequency wind speed sub-series has short-term dependence, whereas the low-frequency sub-series has short-term and long-term dependence. Qu et al.Authors in [48] employed a principal components analysis (PCA) to extract valid information from NWP and input it into LSTM for prediction. It is proposed that Adaptive LSTM uses the Pearson analysis to extract strong correlation factors and input them into LSTM for prediction [49]. In [50] a EEMD-GPR-LSTM method is designed, where ensemble empirical mode decomposition (EEMD) is adopted to decompose the original data of the wind

speed. Afterwards, the LSTM and GPR methods are used to predict the inherent mode functions, respectively. Finally, determine the weight of the two prediction results by the variance-covariance method and provide combined prediction results. In [50], SSA, CEEMDAN and invert-EMD were adopted to reduce noise and decompose the original data and then used the master-slave forecast model composed of ConvLSTM and BPNN to make predictions. The test results showed that the prediction accuracy is competitive. In [51], an E-D LSTM model was proposed to lower specification risk. This model uses the LSTM- based (encoder-decoder) E-D model to build an automatic encoder to map wind power time series to a fixed-length form. Then, enter multiple LSTMs together with weather forecast information to make predictions

Stochastic optimization strategies, which employ supervised learning techniques to learn predictions in the stochastic situation of ED/DCOPF models, are also included in the literature.

For distributed non-linear multi-objective ED, the authors in [12] employed stochastic model predictive control (MPC), which incorporates unpredictable realizations from energy price, renewable resource availability, and demand and employs data-driven scenario development through dynamic programming. A distinct study in [13] used stochastic MPC with data-driven scenario creation and dynamic programming for centralized ED at various time horizons, incorporating demand behavior, energy price uncertainty realizations, and renewable resource availability.

In [14], the authors used Monte Carlo (MC) simulation and the Roulette wheel mechanism (RWM) to construct centralized stochastic MPC for a

contingency-constrained demand response (DR) issue. They included uncertainty realizations from the demand behavior and the availability of renewable resources. By including uncertainty realizations from the availability of renewable resources, the authors in [15] created a centralized stochastic MPC employing probability distribution functions (PDFs) for multi-objective ED with many types of energy sources in a microgrid. In [16], the authors used the Markov chain Monte Carlo (MCMC) approach to present a centralized stochastic MPC method for a multi-objective DR issue, incorporating uncertainty realizations from consumer demand and wind resource availability.

Using Monte Carlo for scenario generation, the authors in [17] suggested centralized stochastic economic MPC for non-linear ED with balance responsible parties (BRPs) by incorporating uncertainty realizations from wind resource availability. By including uncertainty realizations from energy price, renewables, and demand, the authors in [18] suggested a centralized stochastic economic hybrid with reference tracking (ERT) MPC with multi-objective ED formulation using sampling-based scenario generation. In [19], the authors used a sampling-based scenario generation approach to propose a stochastic ERT MPC for multi-objective ED by incorporating uncertainty realizations from energy price and demand.

A centralized stochastic economic MPC for ED was proposed by the authors in [20], who used Gaussian process (GP) regression for uncertainty propagation. In [21], the authors included demand, weather, and electricity prices as uncertain variables in order to present a centralized stochastic economic MPC for a non-linear multi-objective ED problem utilizing scenario-based uncertainty propagation.

For different kinds of ED targets, the aforementioned approaches employed distinct stochastic MPC programming techniques. In all of the aforementioned works, the use of stochastic MPC techniques improved the ED optimal decision and performed better than deterministic MPC. However, the real-time use of the stochastic MPC and stochastic-robust MPC algorithms may be hindered by their substantial computing demands. Furthermore, the stochastic approaches are SLO-based and lack the ability to adjust judgments in order to develop predictions that favor better choices.

An alternative approach to predict unknown parameters is the ILO methodology that focuses on training prediction models to minimize the cost of inaccurate decisions, rather than inaccurate predictions. The application of ILO to optimization problems, and specifically to energy related problems, is scarce in the literature.

For the type shortest path problems, the authors developed a differentiable regret function in [27]. This regret function is non-differentiable for ILO training and resembles a zero-one loss. To make the non-differentiable regret function differentiable, the authors imposed a convex upper-bound on it. They called their training system Smart Predict Then Optimize Plus (SPO+). Using logarithmic barrier relaxation, the authors in [28] suggested a gradient computation based on the interior point (IP) approach for the non-differentiable ILO loss functions of the shortest path, unit commitment, and 0-1 knapsack problems. ILO was primarily employed in the aforementioned experiments to train unknown parameters in the objective function.

The authors in [29] suggested use an IP-based gradient calculation of loss function to train unknown parameters in the constraints. For two types of lin-

ear programming (LPs), packing LP and covering LP, the authors suggested generic gradient formulations. The authors trained unknown parameters in the fractional knapsack problem, alloy production problem, and max flow transportation issue using their gradient formulation. By estimating wind forecasts to optimize decisions rather than wind prediction accuracy, the authors of [30] presented an end-to-end wind power prediction approach to optimize the energy system. The authors of [31] employed decision-focused learning for combinatorial optimization; however, their learning methodology was founded on decision rule optimization (DRO), which parametrizes the choice/policy as well as the unknowns in the optimization model. The optimization model may not accurately reflect the choice or policy since it is an unknown that was learned in conjunction with another unknown. In order to avoid calculating the gradient of the regret function at each epoch, the authors in [32] suggested an end-to-end approach utilizing an energy-based model. They then applied the approach for load prediction in power systems.

The aforementioned works did not develop an ILO for DCOPF that took into account the correlations, sensitivity analysis, influence at various phases of market applications, and ILO training formulations of multiple unknown parameters (load and renewable projections) in the constraints.

To the best of our knowledge, in this work, we develop a novel ILO formulation to achieve an economic operation in both non-real time generator scheduling and real-time market operations. In the limits of ED/DCOPF formulations, the ILO formulation is intended to capture the real-time market and generator scheduling processes for use as feedback for training specific unknown parameters. A new ILO formulation for DCOPF was created to

acquire hour-ahead and real-time cost-effective economic market operations, while the ILO formulation for ED was created primarily to obtain real-time cost-effective market operations. The results show that ILO performs much better than SLO when compared to the SLO-based training of ED/DCOPF unknowns in terms of both training and assessment.

2. Optimal dispatch and real time market operations

The mathematical formulations for optimal dispatch as well as real-time market operations considered in this work are described in this section.

2.1. Economic Dispatch and DC Optimal Power Flow

The focus of the ED optimization problem is the optimal way to allocate resources to meet consumer demand for electricity while satisfying various system-wide restrictions at the lowest possible generation cost. The ED optimization problem is formulated as

$$\min_{p,\, s} \; c^\top p + c^{\text{ext}\top} s, \tag{1a}$$

$$\text{s.t. } 1^\top p + s = 1^\top d, \tag{1b}$$

$$p \le p^{\max}, \tag{1c}$$

$$-p \le -p^{\min}, \tag{1d}$$

$$R \le R^{\max}, \tag{1e}$$

$$-R \le -R^{\min}, \tag{1f}$$

$$-s \le 0, \tag{1g}$$

where $p \in \mathbb{R}^{|\mathcal{I}|}$ denotes the power output of generators, $R \in \mathbb{R}^{|\mathcal{I}|}$ denotes the power output of renewable, $s \in \mathbb{R}$ is the additional power required from an

external system, $c \in \mathbb{R}^{|\mathcal{I}|}$ represents the generation costs, $c^{\text{ext}} \in \mathbb{R}$ is the cost of the external power, $d \in \mathbb{R}^{|\mathcal{B}|}$ represents the load at each bus, 1 is a vector with ones with the proper dimension, $p^{\min}$, $p^{\max} \in \mathbb{R}^{|\mathcal{I}|}$ represent the minimum and maximum generator power output limits, and $R^{\min}$, $R^{\max} \in \mathbb{R}^{|\mathcal{I}|}$ represent the minimum and maximum renewable generation power output limits respectively.

The problem (1) is resolved for every hour of the day, with each hour being defined by a particular context, such as the time of day, the day of the year, the weather, or other pertinent characteristics. It is necessary to forecast the load demand and renewable generation as a function of the context for every hour as the context affects both of these factors. We denote the parameters that depend on the context as unknown parameters, while $c^{\top}$, c^{ext}, $p^{\min}$, $p^{\max}$ do not depend on the context, and thus, they are denoted as known parameters.

2.2. Real time market operations

The current work studies the grid side operations where an ISO balances supply-demand deviations from market clearing schedules in RTM and minimize line-congestion by ramping-up and -down generators. Prior to RTM, the DAM is cleared providing day-ahead set-points that along with other predictions provided by the ISO are applied in ED/DCOPF formulations to generate power dispatching decisions. The prediction-driven ED/DCOPF decision deviates from the true decision due to deviations in prediction. The deviations in load and renewable prediction mainly result in supply-demand imbalance and effects the ramping costs. The ISO corrects deviations in prediction-driven decisions by interacting with real-time market participants

willing to ramp-up/-down their generators for supply-demand balancing. The ISO solves the ED/DCOPF problems to supply consumer loads by scheduling different generators using load prediction while also controlling renewable predictions which minimizes ramping costs further. After the true load and renewable are known, the ISO corrects supply-demand imbalances by ramping-up or -down different generators in the market at prices different than the day-ahead market clearing price (MCP). The renewable control significantly enhances the effect of load-imbalancing thereby providing ease for generator ramping and minimizing ramping costs. The ISO also trades electricity with different regions if the generators within the same region cannot ramp-up/-down corresponding to prediction inaccuracies.

Due to price differences from MCP, the demand participants are subjected to extra payments (indirect penalty due to generator ramping) for both over and underestimations in the load. Moreover, renewable energy predictions if not controlled to be within a specific region of optimality may lead to further increase in market ramping costs. The current study thus, instead of minimizing load and renewable prediction errors, minimizes extra payments on demand participants as a result of generator ramping due to inaccurate load and renewable predictions using ILO. The ILO as explained in the upcoming sections integrates learning and optimization to capture ISO real-time correction procedures to be used as a feedback to learn the load and renewable predictions to minimize extra payments on demand participants. The functioning of the system under study is illustrated in Fig. 1.

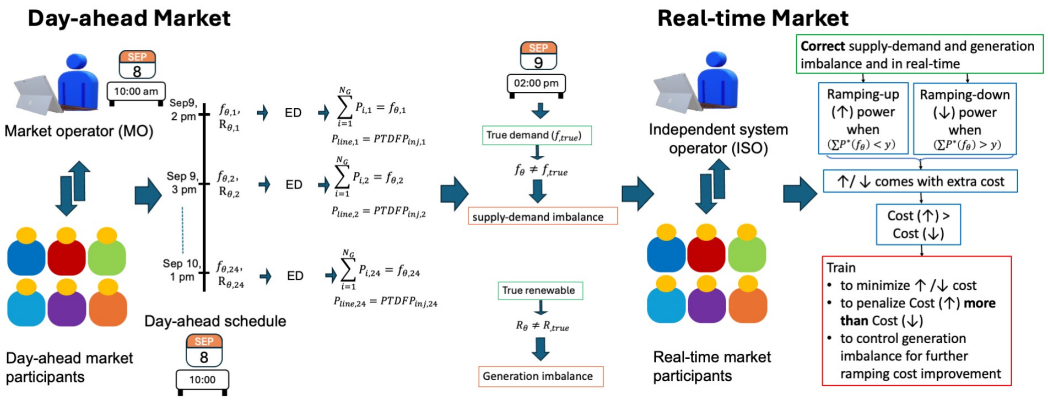

Figure 1: Two markets namely the day ahead market (DAM) and the real-time market (RTM). The market operator (MO) interacts with market participants in the DAM to schedule load and generators for next 24 hours ahead of that day (shown in Fig., say at 8 Sept., 10 am the MO schedules the loads for the next 24 hours starting from 9 Sept., 2 pm). The predicted renewable (R_θ) and load (f_θ) are provided by supply and demand participants. The true load (f_{true}) and true renewable (R_{true}) are realized in real-time and do not match the predicted load and PTDF. The ISO interacts with the market participants to correct load imbalance in real-time. Inspired by the above-mentioned process, we use ILO training pipeline to train load and renewable predictions to minimize ramping-up(↑)/ramping-down(↓) costs, penalize ↑ more than ↓, and control renewable predictions to further optimize the ramping costs.

3. Integrated learning and optimization methodology

Three steps are commonly used to solve Problem (1) with unknown parameters: first, prediction models are trained; second, the unknown parameters, d and R, are predicted using the models trained in the first phase; and third, the optimization problem is solved using the predictions. Because the three phases are solved sequentially without a feedback loop from the post-optimization results to the prediction phase, this method is known as SLO.

Consider a linear program with the general formulation

$$z^*(y) := \min_x \; c^\top x, \tag{2a}$$

$$\text{s.t. } g(x, y) \leq 0, \tag{2b}$$

where $x \in \mathbb{R}^n$ is a vector of decision variables, $c \in \mathbb{R}^n$ is a vector of known parameters, $g : \mathbb{R}^n \to \mathbb{R}^m$ represents a set of m constraints, $y \in \mathbb{R}^m$ is a vector of unknown parameters that depend on the context, and $z \in \mathbb{R}$ is parameterized over y. Problem (2) captures the structure of Problem (1) in terms of variables, constraints, and parameters.

Generally speaking, the prediction models used in the first stage employ a strategy that reduces the forecast errors relative to the actual (or realized) values. Take the prediction of the parameter y that is dependent on a context denoted by A, for instance, using a prediction model that consists of the following elements: [27]:

1. Historical training data is available represented by $\{(A_1, y_1), ..., (A_I, y_I)\}$, mapping contextual information, $A_i \in \mathbb{R}^{m \times n}$, with the corresponding realizations of y.

2. A hypothesis class $\mathcal{H}$ of prediction models $f : \mathcal{X} \to \mathbb{R}^d$, where the predicted unknown parameter, $\hat{y}$, is a function of the context: $\hat{y} := f(A)$.
3. A loss function $l : \mathbb{R}^d \times \mathbb{R}^d \to \mathbb{R}_+$ that quantifies the error of the prediction $\hat{y}$ in respect to the true value of y. For example, this loss function can be a least square loss function.
4. Given the training data and the loss function, by the Empirical Risk Minimization (ERM) principle a prediction model $f^* \in \mathcal{H}$ is determined by

$$f^* := \underset{f \in \mathcal{F}}{\operatorname{argmin}} \frac{1}{I} \sum_{i=1}^{I} l[f(A_i), y_i]. \tag{3}$$

Following the determination of f^* in the first phase of the sequential learning and optimization technique, the prediction $\hat{y} := f^*(\hat{A})$ for a given context $\hat{A}$ is computed in the second phase, and $\hat{y}$ is then used to solve the optimization problem (2).

Using the ERM principle to train model parameters θ by backpropagating the gradient of the loss function, the prediction output $f^i_\theta(A^i)$ is computed to minimize estimation error with respect to true value (y) for a given i^{th} context A^i. This summarizes the SLO pipeline in Figure 2(a). The pipeline is made sequential (predict and optimize sequentially) by using the learned $f^i_\theta(A^i)$ to solve the optimization problem in the following phase. (4) is then utilized to further check the pipeline's quality.

In the SLO approach, in a post-optimization phase and after collecting the following information:

1. the realization of y;
2. the decisions $x^*(\hat{y})$ obtained from the optimization problem (2);

3. the decisions $x^*_{corr}(\hat{y})$ implemented in reality; and

4. the optimum decisions $x^*(y)$ calculated after the realization of y;

the prediction $\hat{y}$ can be assessed using a loss function (regret function) defined

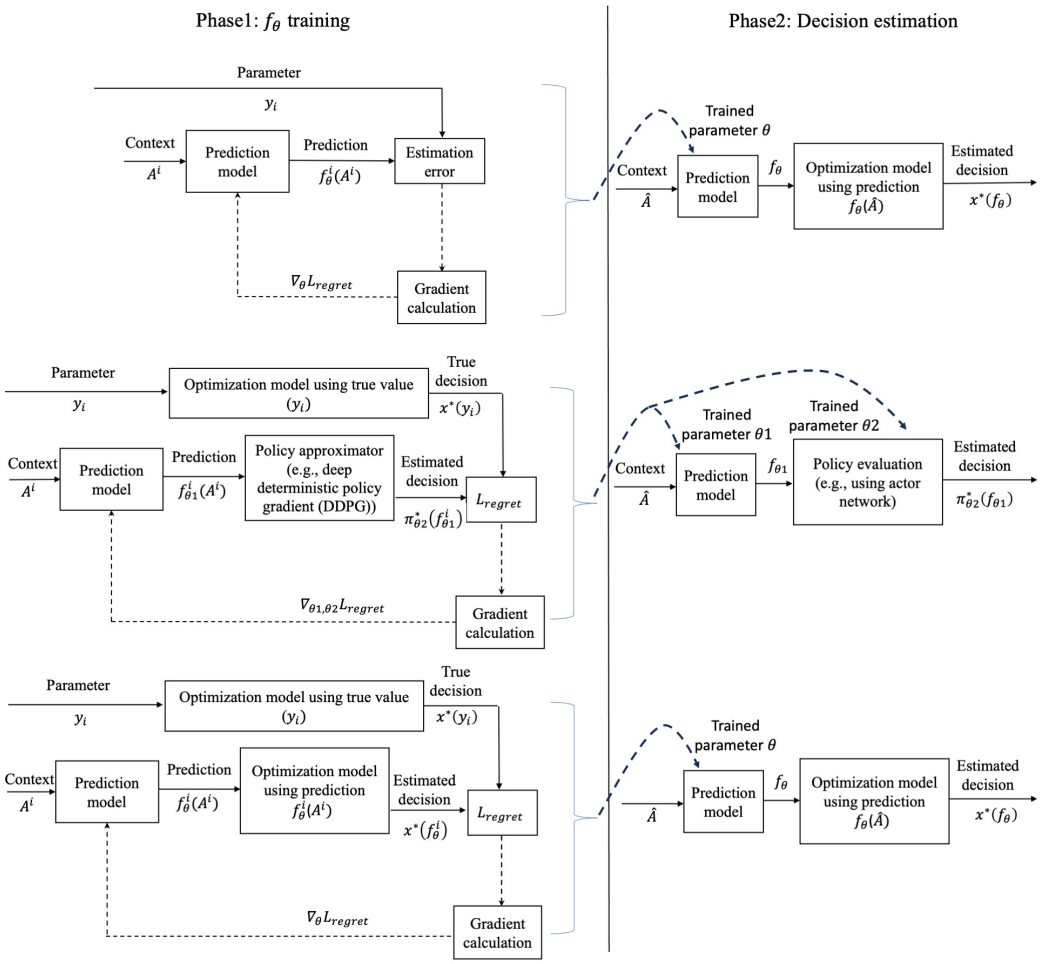

Figure 2: Comparison between different training pipelines, (a) Sequential learning and optimization (SLO), (b) Integrated learning and optimization (ILO), and (c) Decision rule optimization (DRO)

as [29, 39]:

$$L(x^*(\hat{y}), y) := \underbrace{c^\top x^*_{corr}(\hat{y}) - z^*(y)}_{\text{Regret term}} + \underbrace{\phi \circ c^\top \left[x^*(\hat{y}) - x^*_{corr}(\hat{y})\right]}_{\text{Penalty term}}, \tag{4}$$

where $z^*(y) := c^\top x^*(y)$ is the minimum cost that could be achieved for the true y, and $x^*(\hat{y})$ is the solution obtained from problem (2). A correction performed to $x^*(\hat{y})$ to adjust to a true y that differs from $\hat{y}$ is the reason behind the decisions $x^*_{corr}(\hat{y})$ implemented. The cost increase of implementing $x^*_{corr}(\hat{y})$ instead of $x^*(y)$ is thus captured by the first term, while the penalty incurred to correct $x^*(\hat{y})$ to $x^*_{corr}(\hat{y})$ is taken into account by the second term. The penalty is represented by ϕ, multiplied element-wise by the cost vector c.

This post-optimization data, or the regret function value, is not used in the SLO to improve predictions. Nonetheless, it is a key element of the ILO. The ILO framework is summarized below, together with notation and formulations derived from [27, 28, 29].

3.1. Integrated learning and optimization

The prediction method discussed in the previous section is expanded in three ways by the proposed ILO methodology (shown in Figure 2(b)): 1) by using historical training data; 2) by incorporating the optimization problem (2) into the prediction method; and 3) by substituting a novel regret function for the loss function.

The historical training data $\{(A_1,\ y_1),\ ...,\ (A_I,\ y_I)\}$ is augmented with $(x^*(y_i),\ z^*(y_i))$, where $x^*(y_i)$ represents the optimal decisions and $z^*(y_i)$ the optimal solution obtained from (2) for $(A_i,\ y_i)$. By integrating an optimization step into the prediction method, the optimal solution $(x^*(f^i_\theta),\ z^*(f^i_\theta))$

can be obtained from problem (2) for the prediction $f_\theta^i(A^i)$. Based on this additional data[1], a new regret function based on (4) is implemented to replace the loss function l. This regret function quantifies the error of the optimal decisions $x^*(f_\theta^i)$ in respect to $x^*(y_i)$, where f_θ is a prediction model parameterized over θ. Note that in the sequential learning and optimization, the loss function quantifies the error of f_θ^i in respect to y_i. To update θ, the gradient of the regret function is evaluated and passed to the prediction algorithm.

The ILO framework for optimization problems with unknown parameters that only exist in the objective function was defined in the work in [27]. The judgments derived from the prediction are viable for any realization of y in this specific example since the feasible region of the optimization problem is independent of the unknown parameter. The loss function should take into consideration the cost of the correction necessary to move the decisions to the feasible region defined by the true y, since the decisions made using the prediction might not be feasible for all realizations of y if the unknown parameters appear in the constraints. For particular applications, the evolution of these corrections has been documented in [28, 29]. Therefore, in (4), we provided an example of a generic regret function that minimizes regret and accounts for infeasibility in the prediction-driven solution $x^*(\hat{y})$ in relation to the genuine solution $(x^*(y))$.

Following the determination of f^*, the optimization problem (2) is solved using the prediction $\hat{y} := f^*(\hat{A})$ for a particular context $\hat{A}$. The same regret

[1]The historical pair $(x^*(y_i), z^*(y_i))$ and the optimal solution $(x^*(f_\theta^i),\ z^*(f_\theta^i))$.

function used in the prediction model can be utilized to measure the forecast's quality in a post-optimization step following the realization of y, just like in the SLO framework.

In this work, we propose a novel loss function that include correction terms for the ED problem and establish a connection between the loss function, correction and the RTM described in Section 2.2

Remark: Though there is another pipeline called decision rule optimization optimization (DRO) (see Fig. 2 (c)), the ILO and SLO pipelines are the focus of the current work. Using policy approximation methods, the DRO pipeline trains the prediction model instances ($f^i_{\theta 1}(A^i)$). The parameters for prediction and policy models are contained in the policy ($\pi^*_{\theta 2}(f^i_{\theta 1})$). Parameters $\theta 1$ and $\theta 2$, which belong to the prediction model and policy model, respectively, are updated by minimizing the related regret function (L).

Based on the above comparisons, the SLO pipeline learns the load prediction model to minimize error concerning the ground truth load. The load prediction model trained accurately used in optimization problem may not yield decisions favouring better power system operations despite good prediction accuracy.

The closest in decision based learning concept to ILO is the DRO pipeline (eg., deep reinforcement learning (DRL)) which, similar to ILO, learns the prediction model to optimize decisions. However, DRO maps the context to an approximated/parameterized decision. The DRO thus involves two approximations, prediction of optimization problem unknowns and prediction of optimization problem decisions. The parametrized DRO decisions learned integratedly with other problem unknowns may not represent the true prob-

lem decisions.

3.2. ILO applied to ED/DCOPF and RTM

The concept of ILO can be extended to train unknown parameters in the ED optimization model using feedback information from real power system operations. The feedback information refers to some output of the power system in response to the prediction-driven decision input to the power system. The ED optimization model has the load demand (say f_{true}) (demand participant load) and renewable generation (say R_{true}) as unknown parameters in the power-balancing equality constraints. The unknown parameters as explained previously are the parameters in the optimization problem setting that depend on the context and need to be estimated/predicted using contextual information before solving the optimization problem.

3.2.1. Post-hoc (a posteriori) Analysis

The load estimation using ILO to minimize RTM operation costs and line congestion is based on the concept of post-hoc analysis. The post-hoc analysis involves correcting decisions corresponding to predictions using real-time true decisions. The post-hoc analysis resembles the real-world decision correction, where a decision taken prior to real-time using prediction differs from the decision made in real-time using true value. The difference between the two decisions is corrected in real-time, which, depending on the application may or may not incur extra correction penalty (extra cost). For model training using ILO, the correction between decisions with or without a penalty constitutes a regret function whose gradient is used to train the model parameters.

For load and renewable training using ILO, the ED problem is initially solved using the load and renewable prediction model. Once the true load and renewable are known in real-time (historical load data during training), the ILO minimizes an objective-specific regret function (L) (minimizing RTM operation costs in the current study). The regret function is minimized by updating load prediction model parameters using gradient descent (GD) which eventually minimizes RTM operation costs as detailed in the upcoming sub-section.

3.2.2. Regret Function Design for ED Applied to RTM

The L for ED load and renewable training as explained previously is based on the concept of minimizing RTM operation costs. In the current study, the RTM operation costs are additional costs (higher than market costs) incurred as a result of generator ramping operations to balance supply-demand in real-time due to inaccurate load predictions. The ramping-up price (bidding price (BP)) and ramping-down price (offer price (OP)) must hold the following relationships with MCP: $BP > MCP$ and $OP < MCP$. These pricing relationships indicate the extra price to be paid by the demand-side market participant for incorrect load estimations to the regulation market participants willing to ramp-up or -down their generation for supply-demand balancing. The regulation market players pay less when buying energy from ISO while charging more when selling energy to the ISO thereby imposing extra price/penalty to the demand participants.

We propose a novel regret function based on (4) and on the following assumptions:

1. $x^*(\hat{y})$ is corrected to optimality, whereby $x^*_{corr}(\hat{y}) = x^*(y)$, and there-

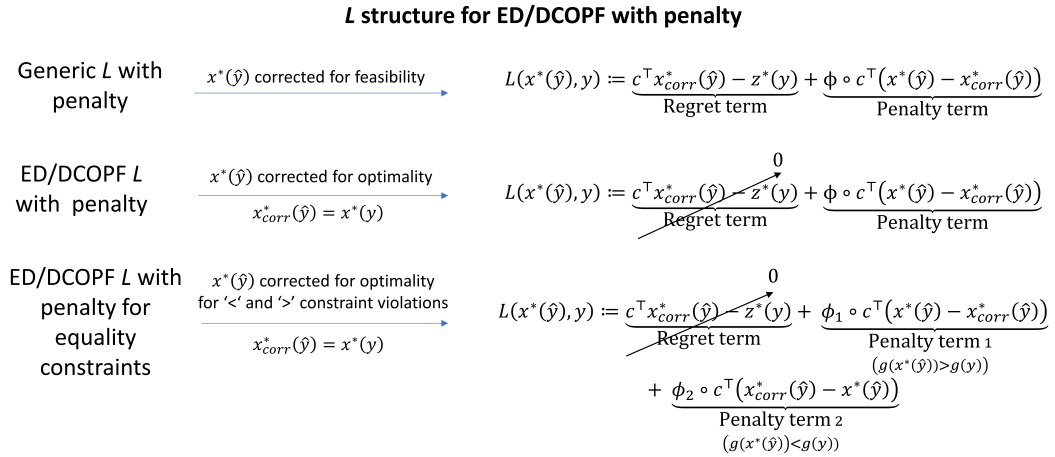

Figure 3: L structure for ED/DCOPF unknown parameter training in equality constraints. The notation used for predictions and true parameters is same as used while explaining generic regret function formulations.

fore, $c^\top x^*_{corr}(\hat{y}) - z^*(y) = 0$.

2. $x^*_{corr}(\hat{y}) = x^*(\hat{y}) + r + s$, where r, $s \in \mathbb{R}^n$ are correction factors needed to bring the system from $x^*(\hat{y})$ to $x^*_{corr}(\hat{y})$.

The first assumption is motivated by the operation of a power system where the power generated is equal to the power consumed. While in the context of the ED and RTM, $r := r^+ - r^-$ where r^+, $r^- \in \mathbb{R}^n_+$ represent the ramp-up and ramp-down power output of generators, , respectively, and $s := s^+ - s^-$ where s^+, $s^- \in \mathbb{R}^n_+$ are the additional power obtained and supplied to neighbor power systems, respectively. With these assumptions and inspired on the extra price/penalty concept, the general structure of L for ILO applied to

ED and RTM is defined as:

$$L = c^{\mathrm{BP}\top} r^{-} + c^{\mathrm{BP,ext}\top} s^{-} + \left(c^{\mathrm{MCP}} \oslash c^{\mathrm{OP}}\right) \circ c^{\mathrm{MCPT}} r^{+} + \left(c^{\mathrm{MCP,ext}} \oslash c^{\mathrm{OP,ext}}\right) \circ c^{\mathrm{MCP,extT}} s^{+}$$

with the following constraints

$$\begin{aligned}
&r^{+} \geq p^{*}(f_{\theta}, R_{\theta}) - p^{*}(f_{true}, R_{true}),\\
&r^{-} \geq p^{*}(f_{true}, R_{true}) - p^{*}(f_{\theta}, R_{\theta}),\\
&s^{+} \geq s^{*}(f_{\theta}, R_{\theta}) - s^{*}(f_{true}, R_{true}),\\
&s^{-} \geq s^{*}(f_{true}, R_{true}) - s^{*}(f_{\theta}, R_{\theta}),\\
&r^{+},\ r^{-} \geq 0,\\
&s^{+},\ s^{-} \geq 0,
\end{aligned} \tag{5}$$

where c^{BP}, c^{OP}, c^{MCP} and $c^{\mathrm{BP,ext}}$, $c^{\mathrm{OP,ext}}$, $c^{\mathrm{MCP,ext}}$ denotes prices to calculate the cost of power ramping-up at BP, cost of power ramping-down at OP, cost of power production at MCP within the same region and power ramping-up at BP, cost of power ramping-down at OP, cost of power production at MCP within the different region respectively. The symbols $\oslash$ and $\circ$ represent the hadamard element-wise division and multiplication of vectors respectively.

The terms $c^{\mathrm{BP}\top} r^{-}$ and $c^{\mathrm{BP,ext}\top} s^{-}$ represent penalty on the demand participants when regulation market players selling power to ISO at higher than MCP. The terms $\left(c^{\mathrm{MCP}} \oslash c^{\mathrm{OP}}\right) \circ c^{\mathrm{MCPT}} r^{+}$ and $\left(c^{\mathrm{MCP,ext}} \oslash c^{\mathrm{OP,ext}}\right) \circ c^{\mathrm{MCP,extT}} s^{+}$ represent penalty to demand participants when regulation market participants purchasing power from ISO at less than MCP. The demand participants here refer to the market participants which provide load prediction prior to real-time.

In both cases, demand participants will be penalized which in other words

also means paying higher than MCP by a certain amount. The above relation thus in terms of cost due to MCP can be written as

$$L := \phi^{+} c^{\mathrm{MCP}\top} r^{+} + \phi^{+\mathrm{ext}} c^{\mathrm{MCP,ext}\top} s^{+} + \phi^{-} c^{\mathrm{MCP}\top} r^{-} + \phi^{-\mathrm{ext}\top} c^{\mathrm{MCP,ext}\top} s^{-}$$

with the following constraints

$$\begin{aligned}
&r^{+} \geq p^{*}(f_{\theta}, R_{\theta}) - p^{*}(f_{true}, R_{true}),\\
&r^{-} \geq p^{*}(f_{true}, R_{true}) - p^{*}(f_{\theta}, R_{\theta}),\\
&s^{+} \geq s^{*}(f_{\theta}, R_{\theta}) - s^{*}(f_{true}, R_{true}),\\
&s^{-} \geq s^{*}(f_{true}, R_{true}) - s^{*}(f_{\theta}, R_{\theta}),\\
&r^{+},\, r^{-} \geq 0,\\
&s^{+},\, s^{-} \geq 0,
\end{aligned} \tag{6}$$

where ϕ^{+} and $\phi^{+\mathrm{ext}}$ represent penalty factors with respect to MCP for ramping-down (corresponding to OP), while the terms ϕ^{-} and $\phi^{-\mathrm{ext}}$ represent the penalty factors with respect to MCP for ramping-up (corresponding to BP).

Generally, the extra price for ramping-up is higher than the amount paid for ramping-down power generation. The L thus, in addition to minimizing the ramping costs for incorrect load estimations is designed to penalize more load underestimations (require ramping-up) compared to load overestimations (require ramping-down). The L concept for ED is illustrated for a two generator example in Figs. 4-8 while the L pipeline is shown in Fig. 9. With renewable, feasible region exhibit more optimality regions.

3.2.3. Gradient for the ED's regret function

To train the load, the L in (6) will be minimized using the ERM principle (3) and the gradient descent (GD) algorithm, which requires calculating the

gradient of L in (6) with respect to unknown parameters θ. To calculate the gradient, (6) is rewritten as

$$\begin{aligned} L := & \phi^{+} c^{\mathrm{MCP}\top} r^{+} \max\left[p^{*}(f_{\theta}, R_{\theta}) - p^{*}(f_{true}, R_{true}), 0\right] \\ & + \phi^{+\mathrm{ext}} c^{\mathrm{MCP,ext}\top} s^{+} \max\left[s^{*}(f_{\theta}, R_{\theta}) - s^{*}(f_{true}, R_{true}), 0\right] \\ & + \phi^{-} c^{\mathrm{MCP}\top} r^{-} \max\left[p^{*}(f_{true}, R_{true}) - p_{i}^{*}(f_{\theta}, R_{\theta}), 0\right] \\ & + \phi^{-\mathrm{ext}} c^{\mathrm{MCP,ext}\top} s^{-} \max\left[s^{*}(f_{true}, R_{true}) - s^{*}(f_{\theta}, R_{\theta}), 0\right]. \end{aligned} \tag{7}$$

The differential to (7) using the total law of derivatives is calculated as

$$\begin{aligned} \nabla_{\theta} L(f_{\theta}, f_{true}, R_{\theta}, R_{true}) := & \frac{\partial L(f_{\theta}, f_{true}, R_{\theta}, R_{true})}{\partial \theta} \\ = & \frac{\partial L(f_{\theta}, f_{true}, R_{\theta}, R_{true})}{\partial p^{*}(f_{\theta}, R_{\theta})} \frac{\partial p^{*}(f_{\theta}, R_{\theta})}{\partial f_{\theta}, R_{\theta}} \frac{\partial f_{\theta}, R_{\theta}}{\partial \theta} + \frac{\partial L(f_{\theta}, f_{true}, R_{\theta}, R_{true})}{\partial s^{*}(f_{\theta}, R_{\theta})} \frac{\partial s^{*}(f_{\theta}, R_{\theta})}{\partial f_{\theta}, R_{\theta}} \frac{\partial f_{\theta}, R_{\theta}}{\partial \theta} \\ = & \left\{ \phi^{+} \frac{\partial c^{\mathrm{MCP}\top} r^{+}}{\partial p^{*}(f_{\theta}, R_{\theta})} \frac{\partial p^{*}(f_{\theta}, R_{\theta})}{\partial f_{\theta}, R_{\theta}} \frac{\max[p^{*}(f_{\theta}, R_{\theta}) - p^{*}(f_{true}, R_{true}), 0]}{p^{*}(f_{\theta}, R_{\theta}) - p^{*}(f_{true}, R_{true})} \right. \\ & \left. + \phi^{+\mathrm{ext}} \frac{\partial c^{\mathrm{MCP,ext}\top} s^{+}}{\partial s^{*}(f_{\theta}, R_{\theta})} \frac{\partial s^{*}(f_{\theta}, R_{\theta})}{\partial f_{\theta}, R_{\theta}} \frac{\max[s^{*}(f_{\theta}, R_{\theta}) - s^{*}(f_{true}, R_{true}), 0]}{s^{*}(f_{\theta}, R_{\theta}) - s^{*}(f_{true}, R_{true})} \right\} \frac{\partial f_{\theta}, R_{\theta}}{\partial \theta} \\ & + \left\{ \phi^{-} \frac{\partial c^{\mathrm{MCP}\top} r^{-}}{\partial p^{*}(f_{\theta})} \frac{\partial p^{*}(f_{\theta})}{\partial f_{\theta}} \frac{\max[p^{*}(f_{true}) - p^{*}(f_{\theta}), 0]}{p^{*}(f_{true}) - p^{*}(f_{\theta})} \right. \\ & \left. + \phi^{-\mathrm{ext}} \frac{\partial c^{\mathrm{MCP,ext}\top} s^{-}}{\partial s^{*}(f_{\theta}, R_{\theta})} \frac{\partial s^{*}(f_{\theta}, R_{\theta})}{\partial f_{\theta}, R_{\theta}} \frac{\max[s^{*}(f_{true}, R_{true}) - s^{*}(f_{\theta}, R_{\theta}), 0]}{s^{*}(f_{true}, R_{true}) - s^{*}(f_{\theta}, R_{\theta})} \right\} \frac{\partial f_{\theta}, R_{\theta}}{\partial \theta}. \end{aligned} \tag{8}$$

The terms $\frac{\partial c^{\mathrm{MCP}\top} r^{-}}{\partial p^{*}(f_{\theta})}$, $\frac{\partial c^{\mathrm{MCP}\top} r^{+}}{\partial p^{*}(f_{\theta})}$, $\frac{\partial c^{\mathrm{MCP,ext}\top} s^{-}}{\partial s^{*}(f_{\theta})}$, and $\frac{\partial c^{\mathrm{MCP,ext}\top} s^{+}}{\partial s^{*}(f_{\theta})}$ in (8) are straightforward to calculate, while the term $\frac{\partial f_{\theta}}{\partial \theta}$ is evaluated using the back-propagation algorithm. The terms $\frac{\partial p^{*}(f_{\theta})}{\partial f_{\theta}}$ and $\frac{\partial s^{*}(f_{\theta})}{\partial f_{\theta}}$ are obtained from an interior point (IP) based sub-gradient calculation, as proposed in [28, 29] (the python code for interior point algorithm was developed using ChatGPT).

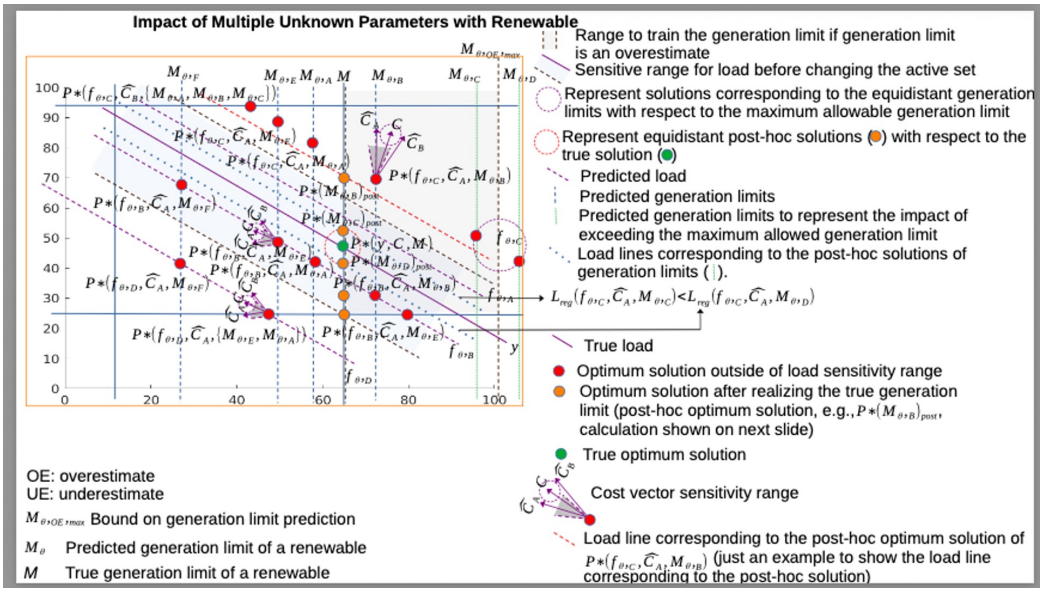

Figure 4: Feasible region explanation

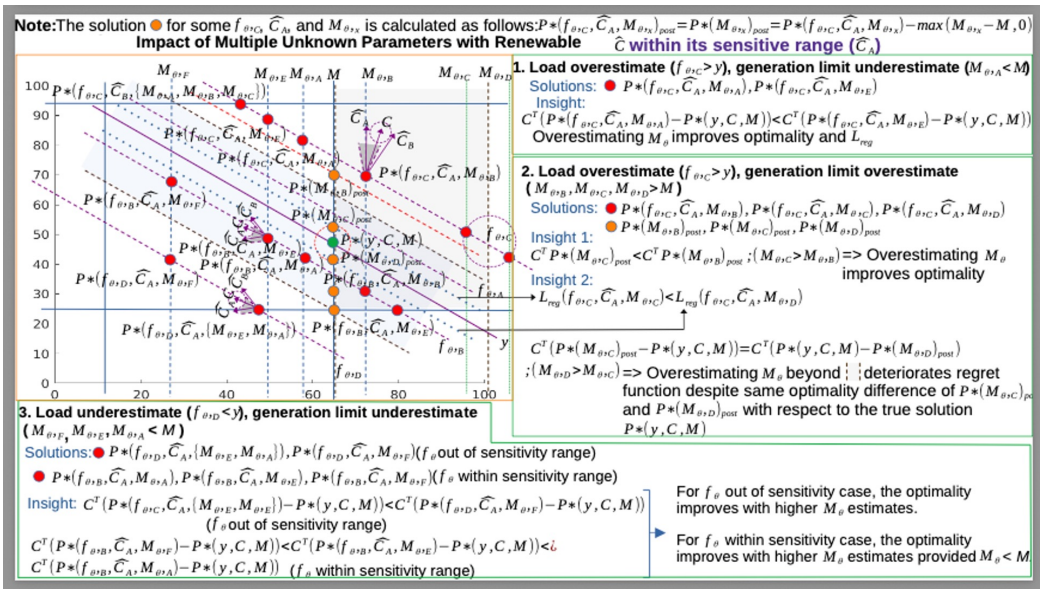

Figure 5: Feasible region explanation

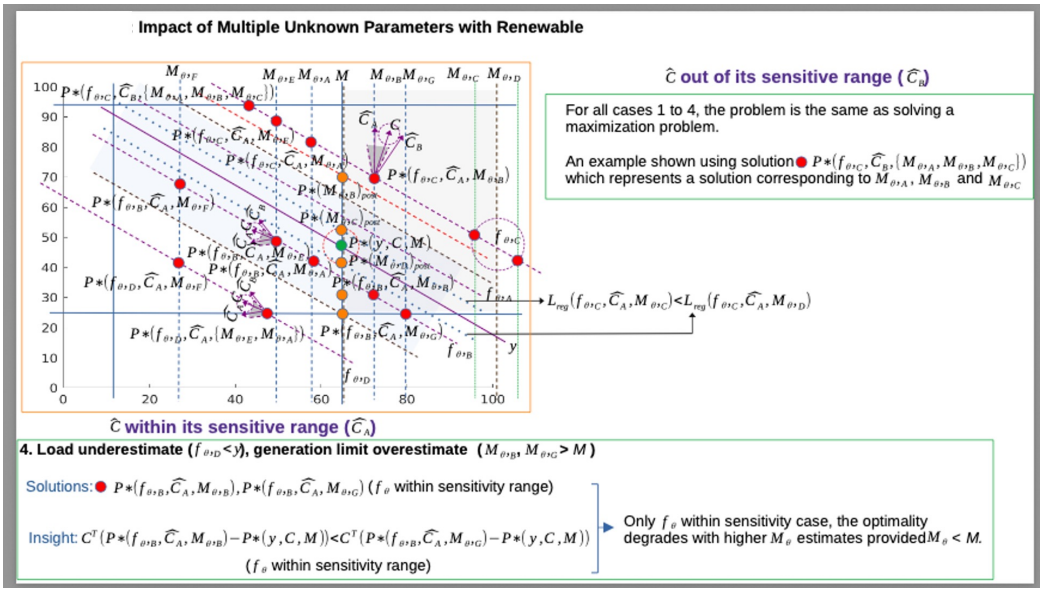

Figure 6: Feasible region explanation

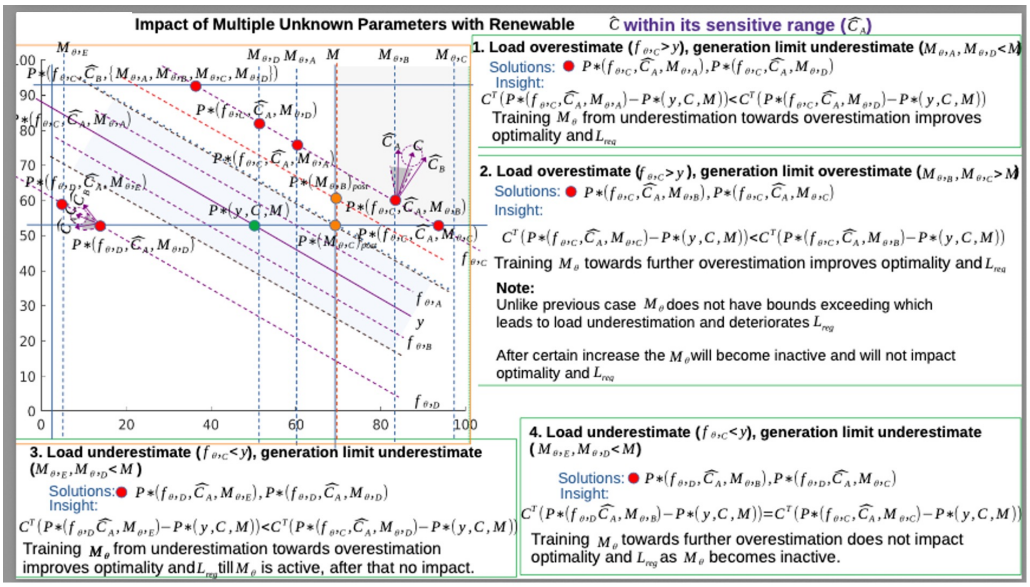

Figure 7: Feasible region explanation

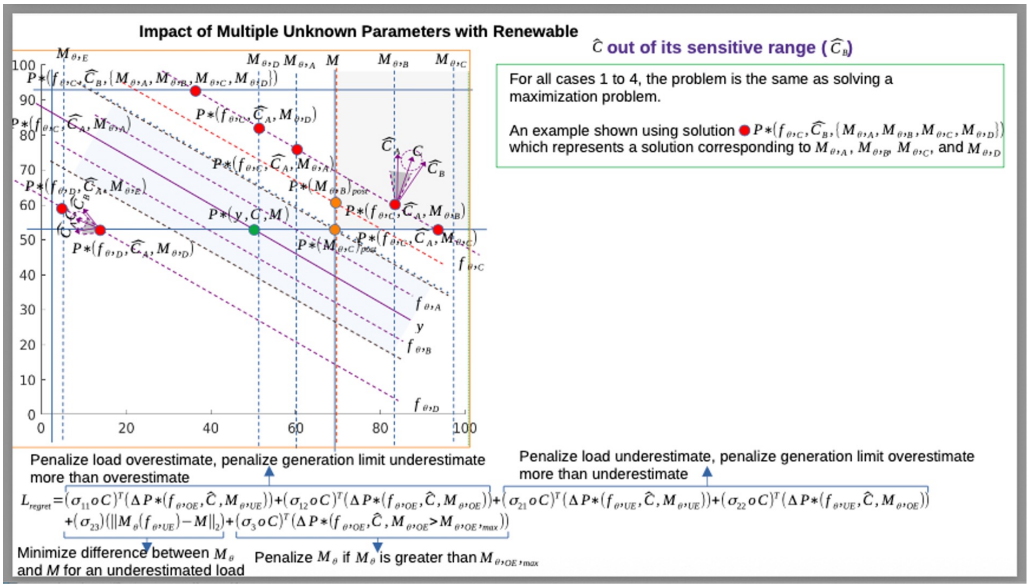

Figure 8: Feasible region explanation

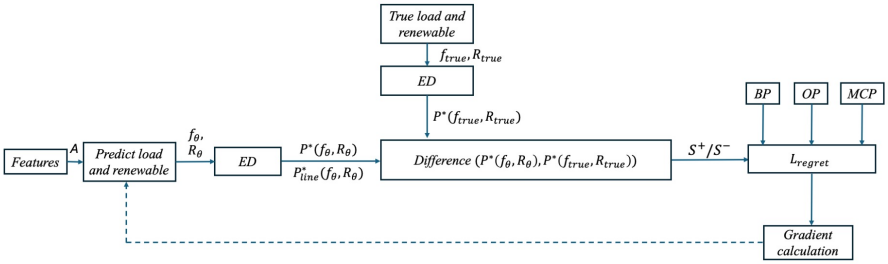

Figure 9: Load and renewable training using ILO. The predicted load (f_θ), predicted renewable (R_θ) and true load (f_{true}), true renewable (R_{true}) are used to solve the DCOPF problem to generate corresponding power set-points $p^*(f_\theta, R\theta)$ and $p^*(f_{true}, R_{true})$ respectively. The difference between the estimated and true power set-points along with the bidding price (BP), offer price (OP), and market clearing price (MCP)) are used to calculate the L. The gradient is calculated using similar procedures as in Section 4 and backward passed to update f_θ and R_θ parameters.

The last two terms are designed as regularization to preserve load distribution at different nodes as a significant deviation in prediction compared to

the true load at a specific line can be impractical.

4. Results

Two case studies are considered using different IEEE test bus systems to show the capability of ILO in learning combined renewable and load predictions to enhance the ramping costs. The two case studies are as follows:

- Case study 1 - The ED is applied to a IEEE-14 bus system with seven generators and eight loads. The case study analyze the impact of 30%, 40%, and 50% renewable in the system. The seven generators in the system have the operating costs of 0, 0, 0, 40, 50, 60, and 70$/MW. The maximum capacities of each generator are $R_{max,1}$, $R_{max,2}$, $R_{max,3}$, 40, 50, and 20 MW respectively for the 30% renewable penetration case where $R_{max,1-3}$ denotes the maximum/predicted value for renewable. For 40 and 50% renewable penetration the generators are replaced accordingly with renewables. The hour-ahead renewable and load predictions were trained to minimize ramping costs. The percentage variation in renewable penetration is to analyze and verify the ILO decision focused training

- Case study 2 - The ED is applied to a IEEE-118 bus system with nineteen generators and eight loads. The case study analyze the impact of 30%, 40%, and 50% renewable in the system. The nineteen generators in the system have the operating costs of 0, 0, 0, 40, 50, 60, ..., 190$/MW. The maximum capacities of each generator are $R_{max,1}$, $R_{max,2}$, $R_{max,3}$, 40, 50, ..., 20 MW respectively for the 30% renewable

penetration case where $R_{max,1-3}$ denotes the maximum/predicted value for renewable. For 40 and 50% renewable penetration the generators are replaced accordingly with renewables. The hour-ahead renewable and load predictions were trained to minimize ramping costs.

The percentage variation in renewable penetration is to first analyze the impact of change in non-convexity patterns of L on the performance of ILO.

The historical data to train loads and renewables both for IEEE-14 and IEEE-118 systems is obtained from independent system operator New England (ISONE) website. The load and renewable data for both the systems was scaled accordindgly. Moreover, for renewable, the wind data for different percentage penetration of renewables was not available and thus was generated by varying wind speeds as a percentage of the actual data.

The python code for bar plots plots was developed using ChatGPT.

4.1. Training setup

A NN with three hidden layers each having 25 neurons is used for both the case studies. For both ED solution, the interior point optimization (IPOPT) solver [39] was used. For model training, the pytorch and functorch libraries in python were used. In case study one, for load and renewable learning for all renewable penetration percentages the learning rates for ILO and SLO were set as 5×10^{-3} and the barrier coefficient (μ) was unbounded and was typically 1×10^{-9} after solving through IPOPT. For second case study, the learning rates for ILO and SLO were set as 1×10^{-4} and 1×10^{-3} and the barrier coefficient (μ) was limited to 1×10^{-7}.

The ILO training results for both case studies are compared with the SLO in terms of L value in order to compare their performance.

4.2. Case Study 1

In the hour-ahead case, the NN output is a single neuron representing the hour-ahead load prediction corresponding to the environmental features/context. The predictions trained with ILO are compared with the predictions trained with SLO to show the effectiveness of ILO in minimizing L or minimizing ramping costs. Both models are trained using the load data for five days while the predictions are tested using the contextual information of the next two days. The training and testing results for case study 1 corresponding to all percentage renewable penetrations are shown in Table 1.

As observed in Table 1, the ILO trained L exhibit smaller values than SLO for both the training and testing instances for all percentage renewable penetrations. This is due to ILO model training focusing on minimizing extra costs on the demand participant, unlike SLO which focuses on minimizing load prediction error. The results for the improvements in the ramping costs are shown in Figs.10-11. The plots are bar and normal plots to show this and this respectively.

4.3. Case Study 2

In this case, the load and renewable are trained at one hour time resolution for an IEEE-118 bus system. Provided the current feature data, the load and renewable are predicted every next hour. The ILO training and testing results are then compared to SLO training and testing results with the

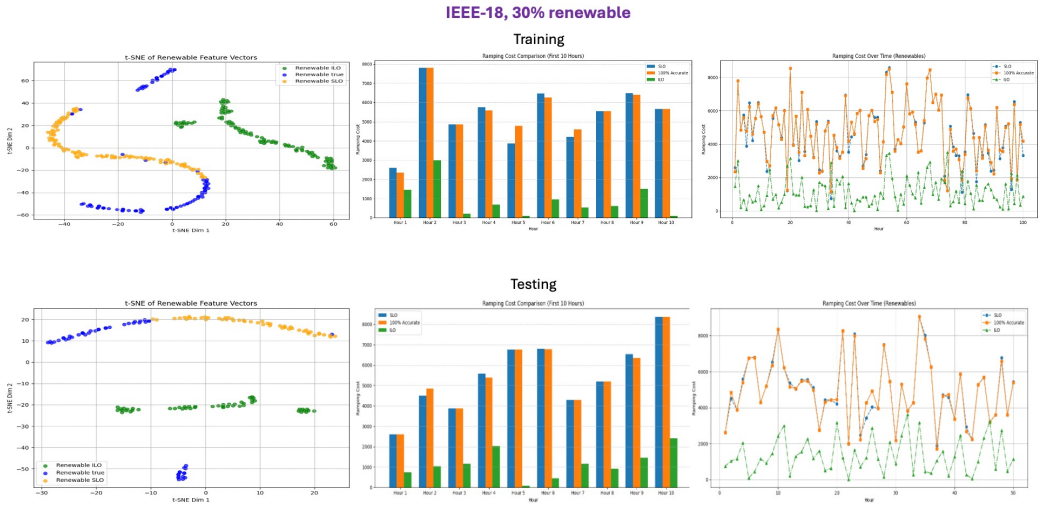

Figure 10: Training and testing results for IEEE-18 bus system with 30% renewable penetration. The tSNE plot represents the predicted values for SLO, true and ILO predictions. The bar plot illustrates the percentage improvements of proposed ILO over SLO and true values for 10 hour operation. The continuous plot represents the complete 5 day operation ramping costs for SLO, true, and ILO.

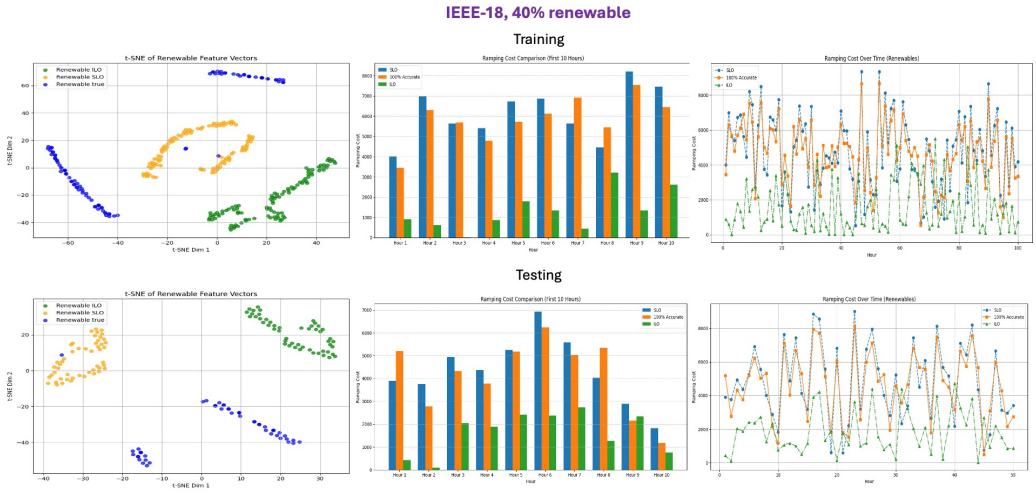

Figure 11: Training and testing results for IEEE-18 bus system with 40% renewable penetration. The tSNE plot represents the predicted values for SLO, true and ILO predictions. The bar plot illustrates the percentage improvements of proposed ILO over SLO and true values for 10 hour operation. The continuous plot represents the complete 5 day operation ramping costs for SLO, true, and ILO.

objective of minimizing the regret function. Table 2 illustrates the comparison between regret functions corresponding to ILO and SLO training. As observed, for all the renewable penetration percentages the regret function of ILO remains smaller than that of SLO. The smaller regret function, as explained previously, enhances economic operation by minimizing real-time correction costs of RTM. To better illustrate the impact of lower L value, Figs.12-14 represents the training and testing results of ramping costs at different hours for all the renewable penetration percentages. The comparison is between ILO, SLO, and 100% accurate renewable prediction. It is clear from the results the ILO based training provide significantly smaller ramping costs compared to both SLO and 100% accurate renewable prediction case. This is due to ILO trained load and renewable when combined follows the optimal region zones explained in Figs.12-14.

5. Conclusion

As a conclusion, the proposed ILO methodology was compared with SLO for ED electricity market parameter training to achieve lower generator ramping costs. For both case study 1 and 2 for all the renewable percentages the ILO outperformed SLO in terms of achieving a lower regret function indicating lower ramping costs. The load trained using ILO for both the case studies was more an overestimate than an underestimate to achieve a lower regret function followed by ILO based decisive control of renewable prediction for further significant enhances in the generator ramping costs.

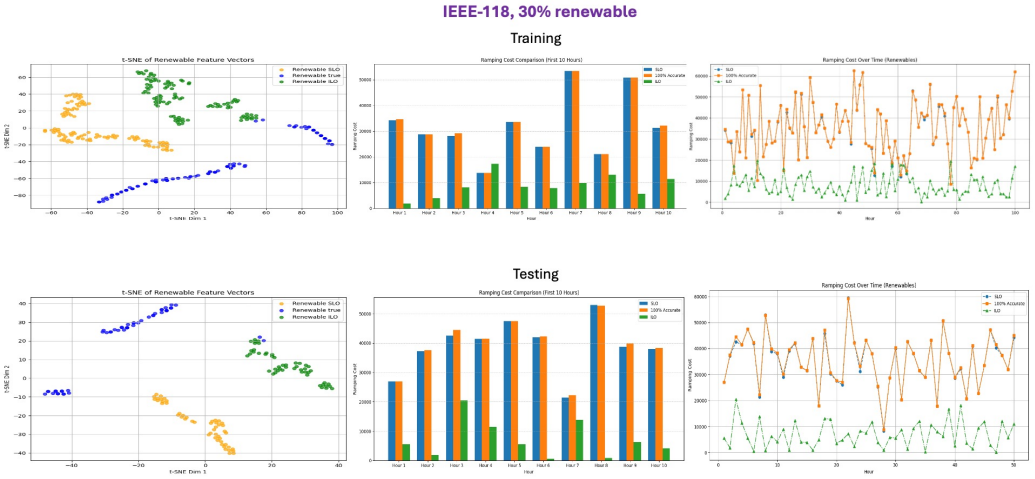

Figure 12: Training and testing results for IEEE-118 bus system with 30% renewable penetration. The tSNE plot represents the predicted values for SLO, true and ILO predictions. The bar plot illustrates the percentage improvements of proposed ILO over SLO and true values for 10 hour operation. The continuous plot represents the complete 5 day operation ramping costs for SLO, true, and ILO.

Notation

Sets

$\mathcal{B}$ - Buses.

$\mathcal{I}$ - Generation units.

$\mathcal{J}$ - Loads.

$\mathcal{L}$ - Transmission lines.

Known parameters[2]

[2]Do not depend on the context.

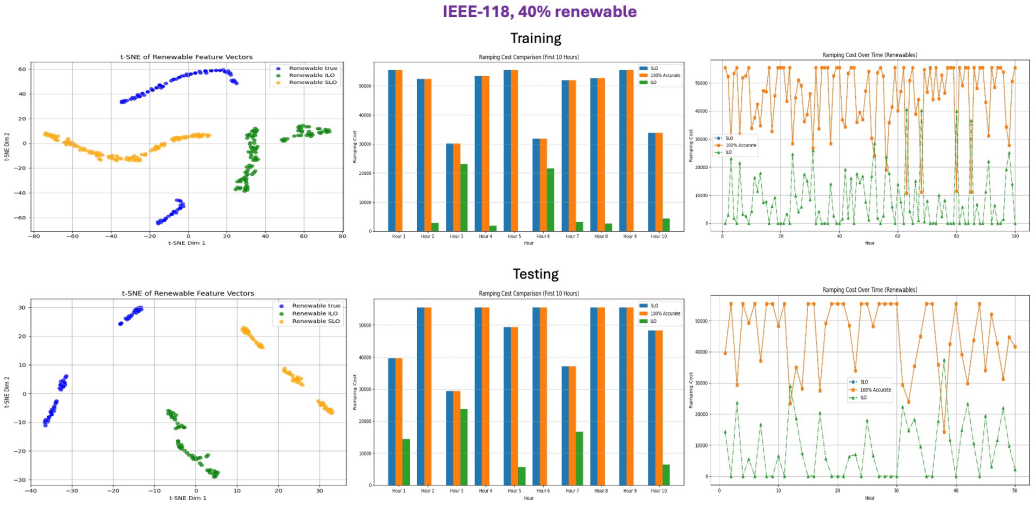

Figure 13: Training and testing results for IEEE-118 bus system with 40% renewable penetration. The tSNE plot represents the predicted values for SLO, true and ILO predictions. The bar plot illustrates the percentage improvements of proposed ILO over SLO and true values for 10 hour operation. The continuous plot represents the complete 5 day operation ramping costs for SLO, true, and ILO.

Unknown parameters[3]

Continuous variables[4]

Abbreviations

ED - Economic dispatch

ERT - Economic hybrid with reference tracking

[3]Depend on the context and need to be predicted as a function of the context.

[4]Obtained as a solution to an optimization problem.

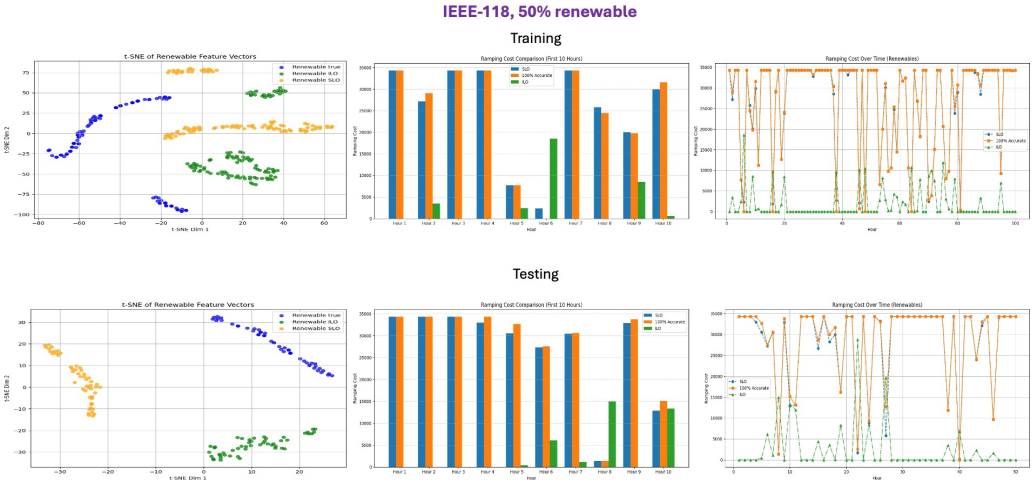

Figure 14: Training and testing results for IEEE-118 bus system with 50% renewable penetration. The tSNE plot represents the predicted values for SLO, true and ILO predictions. The bar plot illustrates the percentage improvements of proposed ILO over SLO and true values for 10 hour operation. The continuous plot represents the complete 5 day operation ramping costs for SLO, true, and ILO.

DAM - Day-ahead market

DCOPF - DC optimal power flow

DRO - Decision rule optimization

DRL - Deep reinforcement learning

IDM - Intra-day market

ILO - Integrated learning and optimization

SPO+ - Smart predict then optimize

ISO - Independent system operator

LO - Learning and optimization

MO - Market operator

MPC - Model predictive control

MCP - Market clearing price

BP - Bidding price

OP - Offer price

NN - Neural network

CNN - Convolutional neural network

LSTM - Long short term memory

LM-BP - Levenberg–Marquardt back-propagation

DCNN - Deep convolutional neural network

GP - Gaussian process

RF - Random forest

GB - Gradient boosting

DP - Dynamic programming

MC - Monte carlo

RWM - Roulette wheel mechanism

DR - Demand response

PDF - Probability distribution function

MCMC - Markov chain Monte Carlo

BRP - Balance responsible party

TFT - temporal fusion transformer

PTDF - Power transfer distribution factor

RTM - Real-time market

SLO - sequential learning and optimization

ISONE - Independent system operator New England

IPOPT - Interior point optimization

IP - Interior point

LP - Linear program

RoCoF - Rate of change of frequency

EV - Electric vehicle

AI declaration statement

During the preparation of this work the author(s) used ChatGPT in order to develop the code for interior point algorithm for DCOPF and verified its performance by comparing it with the actual results. Moreover, the code for generating bar plots and tsne plots was also developed using chatGPT. After using this tool/service, the author(s) reviewed and edited the content as needed and take(s) full responsibility for the content of the publication.

References

[1] Sadana U., Chenreddy A., Delage E., Forel A., Frejinger E., Vidal T., A survey of contextual optimization methods for decision- making under uncertainty. European Journal of Operational Research 320 (2), (2025), pp. 271–289.

[2] Ye, Z.; Kim, M.K. Predicting electricity consumption in a building using an optimized back-propagation and Levenberg-Marquardt back-propagation neural network: Case study of a shopping mall in China. Sustain. Cities Soc. 2018, 42, 176–183.

[3] Wang, C.; Baratchi, M.; Back, T.; Hoos, H.H.; Limmer, S.; Olhofer, M. Towards Time-Series Feature Engineering in Automated Machine Learning for Multi-Step-Ahead Forecasting. Eng. Proc. 2022, 18, 8017.

[4] López-Santos, M.; Díaz-García, S.; García-Santiago, X.; Ogando-Martínez, A.; Echevarría-Camarero, F.; Blázquez-Gil, G.; Carrasco-Ortega, P. Deep Learning and transfer learning techniques applied to short-term load forecasting of data-poor buildings in local energy communities. Energy Build. 2023, 292, 113164.

[5] Fan, C.; Xiao, F.; Zhao, Y. A short-term building cooling load prediction method using deep learning algorithms. Appl. Energy 2017, 195, 222–233.

[6] Khan, S.; Javaid, N.; Chand, A.; Khan, A.B.M.; Rashid, F.; Afridi, I.U. Electricity Load Forecasting for Each Day of Week Using Deep CNN. Adv. Intell. Syst. Comput. 2019, 927, 1107–1119.

[7] Rafi, S.H.; Al-Masood, N.; Deeba, S.R.; Hossain, E. A Short-Term Load Forecasting Method Using Integrated CNN and LSTM Network. IEEE Access 2021, 9, 32436–32448.

[8] Dab, K.; Agbossou, K.; Henao, N.; Dubé, Y.; Kelouwani, S.; Hosseini, S.S. A compositional kernel based gaussian process approach to day-ahead residential load forecasting. Energy Build. 2022, 254, 111459.

[9] Zeyu, W.; Yueren, W.; Rouchen, Z.; Srinivasan, R.S.; Ahrentzen, S. Random Forest based hourly building energy prediction. Energy Build. 2018, 171, 11–25.

[10] Touzani, S.; Granderson, J.; Fernandes, S. Gradient boosting machine for modelling the energy consumption of commercial buildings. Energy Build. 2018, 158, 1533–1543.

[11] Zhong, H.; Wang, J.; Jia, H.; Mu, Y.; Lv, S. Vector field-based support vector regression for building energy consumption prediction. Appl. Energy 2019, 242, 403–414.

[12] Muhammad Bakr Abdelghany, Ahmed Al-Durra, Hatem Zeineldin, Fei Gao, Integrating scenario-based stochastic-model predictive control and load forecasting for energy management of grid-connected hybrid energy storage systems, International Journal of Hydrogen Energy, Volume 48, Issue 91, 2023.

[13] Miguel A. Velasquez, Nicanor Quijano, Angela I. Cadena, Mohammad Shahidehpour, Distributed stochastic economic dispatch via model predictive control and data-driven scenario generation, International Journal of Electrical Power & Energy Systems, Volume 129, 2021.

[14] Farzad Arasteh, Gholam H. Riahy, MPC-based approach for online demand side and storage system management in market based wind integrated power systems, International Journal of Electrical Power & Energy Systems, Volume 106, 2019.

[15] Mostafa Yousefi Ramandi, Nooshin Bigdeli, Karim Afshar, Stochastic economic model predictive control for real-time scheduling of balance responsible parties, International Journal of Electrical Power & Energy Systems, Volume 118, 2020.

[16] J. Lee et al., "Optimal Operation of an Energy Management System Using Model Predictive Control and Gaussian Process Time-Series Modeling," in IEEE Journal of Emerging and Selected Topics in Power Electronics, vol. 6, no. 4, pp. 1783-1795, Dec. 2018, doi: 10.1109/JESTPE.2018.2820071.

[17] DU, Y., PEI, W., CHEN, N.et al.Real-time microgrid economic dispatch based on model predictive control strategy.J. Mod. Power Syst. Clean Energy 5, 787–796 (2017).

[18] F. Garcia-Torres, C. Bordons, J. Tobajas, R. Real-Calvo, I. Santiago and S. Grieu, "Stochastic Optimization of Microgrids With Hybrid Energy Storage Systems for Grid Flexibility Services Considering Energy Forecast Uncertainties," in IEEE Transactions on Power Systems, vol. 36, no. 6, pp. 5537-5547, Nov. 2021, doi: 10.1109/TPWRS.2021.3071867.

[19] M Nassourou, V Puig, J Blesa, Robust Optimization based Energy Dispatch in Smart Grids Considering Simultaneously Multiple Uncertainties: Load Demands and Energy Prices, IFAC-PapersOnLine, Volume 50, Issue 1, 2017.

[20] Gan, L.K.; Zhang, P.; Lee, J.; Osborne, M.A.; Howey, D.A. Data-Driven Energy Management System With Gaussian Process Forecasting and MPC for Interconnected Microgrids. IEEE Trans. Sustain. Energy 2021, 12, 695–704.

[21] Vasilj, J.; Gros, S.; Jakus, D.; Zanon, M. Day-ahead scheduling and real-

time Economic MPC of CHP unit in Microgrid with Smart buildings. IEEE Transactions on Smart Grid 2017,10, 1992–2001.

[22] Zhicheng Liu, Yipeng Liu, Hao Xu, Siyang Liao, Kefan Zhu, Xinxiong Jiang, Dynamic economic dispatch of power system based on DDPG algorithm, Energy Reports, 2022.

[23] Ting Yang, Liyuan Zhao, Wei Li, Albert Y. Zomaya, Dynamic energy dispatch strategy for integrated energy system based on improved deep reinforcement learning, Energy, 2021.

[24] Xiang Zhou, Jiye Wang, Xinying Wang, Sheng Chen, Optimal dispatch of integrated energy system based on deep reinforcement learning, Energy Reports, 2023.

[25] Xinyue Wang, Haiwang Zhong, Guanglun Zhang, Guangchun Ruan, Yiliu He, Zekuan Yu, Adaptive look-ahead economic dispatch based on deep reinforcement learning, Applied Energy, Volume 353, Part B, 2024.

[26] Bongo Y (1997) Using a financial training criterion rather than a prediction criterion. International Journal of Neural Systems 8(4):433–443.

[27] Elmachtoub, Adam N. and Grigas, Paul, Smart "Predict, then Optimize", Manage. Sci., 2022.

[28] Jayanta Mandi and Tias Guns. Interior point solving for LP-based prediction+optimisation. Advances in Neural Information Processing Systems, 33:7272–7282, 2020.

[29] Xinyi Hu, Jasper C.H. Lee, and Jimmy H.M. Lee., "Predict+Optimize for packing and covering LPs with unknown parameters in constraints", Proceedings of the Thirty-Seventh AAAI Conference on Artificial Intelligence, 2023.

[30] Dariush Wahdany, Carlo Schmitt, Jochen L. Cremer, More than accuracy: end-to-end wind power forecasting that optimises the energy system, Electric Power Systems Research, Volume 221, 2023.

[31] Wilder, Bryan, Bistra Dilkina, and Milind Tambe. "Melding the data-decisions pipeline: Decision-focused learning for combinatorial optimization." Proceedings of the AAAI Conference on Artificial Intelligence. Vol. 33. No. 01. 2019.

[32] Kong, Lingkai, et al. "End-to-end stochastic optimization with energy-based model." Advances in Neural Information Processing Systems 35 (2022): 11341-11354.

[33] Šošić, Darko & Škokljev, Ivan & Pokimica, Nemanja. (2014). Features of Power Transfer Distribution Coefficients in power System Networks.

[34] H. Ronellenfitsch, M. Timme and D. Witthaut, "A Dual Method for Computing Power Transfer Distribution Factors," in IEEE Transactions on Power Systems, vol. 32, no. 2, pp. 1007-1015, March 2017, doi: 10.1109/TPWRS.2016.2589464.

[35] Rui, X., Sahraei-Ardakani, M., Nudell, T.R.: Linear modelling of series FACTS devices in power system operation models. IET Generation, Transmission and Distribution 16, 1047–1063 (2022).

[36] Ban H. Alajrash, Mohamed Salem, Mahmood Swadi, Tomonobu Senjyu, Mohamad Kamarol, Saad Motahhir, A comprehensive review of FACTS devices in modern power systems: Addressing power quality, optimal placement, and stability with renewable energy penetration, Energy Reports, Volume 11, 2024, Pages 5350-5371.

[37] M.N. Iqbal, A. Mahmood, A. Amin, H. Arshid, Voltage regulation and power loss minimization by using unified power flow control device, 2019 International Conference on Engineering and Emerging Technologies (ICEET), IEEE (2019), pp. 1-9.

[38] A. Narain, S. Srivastava, An Overview of Facts Devices used for Reactive Power Compensation Techniques, power, vol. 2 (2015), p. 3.

[39] L.T. Biegler. Nonlinear Programming: Concepts, Algorithms and Applications to Chemical Processes. SIAM, Philadelphia, 2010.

[40] Wu, Z., et al.: A comprehensive review on deep learning approaches in wind forecasting applications. CAAI Trans. Intell. Technol. 7(2), 129–143 (2022). https://doi.org/10.1049/cit2.12076

[41] Yang, T., et al.: A novel method of wind speed prediction by peephole LSTM. In: 2018 International Conference on Power System Technology (POWERCON), pp. 364–369. IEEE (2018)

[42] Yu, R., et al.: LSTM-EFG for wind power forecasting based on sequential correlation features. Future Generat. Comput. Syst. 93, 33–42 (2019)

[43] Zhang, Z., et al.: Wind speed prediction method using shared weight long short-term memory network and Gaussian process regression. Appl. Energy. 247, 270–284 (2019

[44] Araya, I.A., Valle, C., Allende, H.: LSTM-based multi-scale model for wind speed forecasting. In: Iberoamerican Congress on Pattern Recognition, pp. 38–45. Springer (2018)

[45] Zhang, Z., et al.: Long short-term memory network based on neighborhood gates for processing complex causality in wind speed prediction. Energy Convers. Manag. 192, 37–51 (2019).

[46] López, E., et al.: Efficient training over long short-term memory networks for wind speed forecasting. In: Iberoamerican Congress on Pattern Recognition, pp. 409–416. Springer (2016).

[47] Xiaoyun, Q., et al.: Short-term prediction of wind power based on deep long short-term memory. In: 2016 IEEE PES Asia-Pacific Power and Energy Engineering Conference (APPEEC), pp. 1148–1152. IEEE (2016).

[48] Xu, G., Xia, L.: Short-term prediction of wind power based on adaptive LSTM. In: 2018 2nd IEEE Conference on Energy Internet and Energy System Integration (EI2), pp. 1–5. IEEE (2018).

[49] Huang, Y., Liu, S., Yang, L.: Wind speed forecasting method using EEMD and the combination forecasting method based on GPR and LSTM. Sustainability. 10(10), 3693 (2018).

[50] Chen, G., et al.: Short-term wind speed forecasting with principle- subordinate predictor based on conv-LSTM and improved BPNN. IEEE Access. 8, 67955–67973 (2020).

[51] Lu, K., et al.: Short-term wind power prediction model based on encoder-decoder LSTM. In: IOP Conference Series: Earth and Environmental Science, vol. 186, p. 012020 (2018).